Melting relations in the system of $MgSiO_3$ –SiO_2 at high pressures

*Takuya Moriguti[1], Akira Yoneda[1], Eiji Ito[1]

1. Institute for Planetary Materials, Okayama University

Melting relations in the MgO–SiO_2 system at high pressures have been extensively studied to simulate chemical differentiation in a deep magma ocean formed in the early stage of the Earth (e.g. Kato and Kumazawa, 1985; Ito and Katsura, 1992). Almost all of these works have been carried out on the compositions ranging from MgO to $MgSiO_3$, assuming that the bulk mantle composition is peridotitic or close to that derived from CI chondrite. Recently enstatite chondrite (E-chondrite) was proposed as the bulk earth source material (Javoy et al., 2010) because the isotope systematics over O, N, Mo, Re, Os, and Cr for the Earth and Moon are almost identical to that of E-chondrite. In E-chondrite, the silicate composition is characterized by $MgO/SiO_2 = 0.5$ (in weight ratio) which is substantially lower than that of the peridotitic mantle (~0.85).
In this context, melting relations on compositions more SiO_2 enriched than $MgSiO_3$ are indispensable to clarify the mantle fraction. However, available information regarding phase relations in the system $MgSiO_3$ –SiO_2 is so far limited to 1 GPa. In the present study, therefore, we would determine the melting relations at pressures 5 to 20 GPa, focusing on the compositions of MgO-xSiO_2 (x = 0.8 to 1.2). We expect to present some new results.

Keywords: enstatite chondrite, melting relation, magma ocean, mantle differentiation, high pressure

Experimental study on the stability and physicochemical behavior of methane hydrate under high pressure and high temperature

*Hirokazu Kadobayashi[1], Hiroaki Ohfuji[1], Hisako Hirai[2], Ohtake Michika[3], Yoshitaka Yamamoto[3]

1. Geodynamics Research Center, Ehime University, 2. Department of Environment Systems, Faculty of Geo-environmental Science, Rissho University, 3. National Institute of Advanced Industrial Science and Technorogy

Methane hydrate are thought to be an important constituent of icy bodies and their satellites, such as Neptune, Uranus and Titan. It is a clathrate compound composed of hydrogen-bonded water cages (host) and molecules or atoms (guests) included in the cages. Methane hydrate has an sI cage structure at low (< 0.8 GPa) pressures and room temperature. It transforms to an sH cage structure at approximately 0.8 GPa, which further transforms to a filled-ice Ih structure at approximately 1.8 GPa. The Ih structure consists of an ice framework similar to ice Ih and voids that are filled with methane molecules (e.g. Loveday et al. 2001; Shimizu et al. 2002). This structure was found to be stable up to at least 86 GPa, supporting that methane hydrate may be stable in the deep interior of icy bodies. Although the sequence of the phase transitions with pressure have been studied well at room temperature, there are only a few studies that addressed the stability of methane hydrate under high pressure and high temperature (Kurnosov et al., 2006; Bezacier et al., 2014). In addition, the pressure range of these previous studies is only limited to < 5 GPa. Therefore, a further investigation is needed to understand the stability and physicochemical behavior of methane hydrate under extreme conditions corresponding to the interior of icy bodies.
In this study, we carefully investigated the stability and decomposition mechanism of methane hydrate in an externally-heated diamond anvil cell in the range of 2-51 GPa and 298-653 K using in-situ Raman spectroscopy and X-ray diffraction. The results show that methane hydrate decomposes to ice VII and solid methane at temperatures considerably lower than the melting curves of solid methane and ice VII in the pressure range of 2-51 GPa. The decomposition conditions of methane hydrate that were obtained at high pressure may help in the modeling of the accretion process and evolutions of icy bodies.

Keywords: methane hydrate, high pressure and high temperature, gas hydrate, diamond anvil cell

Spin transition and thermal conductivity anisotropy of siderite under high pressure

*Keng-Hsien Chao[1,2], Wen-Cheng Owen Huang[1], Wen-Pin Hsieh[2]

1. National Central University, Taiwan, 2. Academia Sinica, Taiwan

Deep carbon cycle plays an important role in controlling the distribution of carbon between Earth’s surface and interior. The subduction slabs transport the carbonates on seafloor into Earth’s interior. Most of the carbons could be trapped in Earth’s interior, and carbons recycled to the ground surface are rare. According to recent studies, Fe-bearing carbonates, for instance siderite, have been considered to be potential carbon hosting minerals inside the Earth’s interior. Previous studies showed that the distribution of Fe-bearing carbonates in mantle is difficult to be detected by seismic observation due to their low concentration, yet there is strong elastic anisotropy in Fe-bearing carbonate which could be a potential diagnostic feature. In addition to their intrinsic elastic anisotropy, spin transition of Fe driven by extremely high pressure is another factor that could change the physical properties of siderite. For instance, the volume of siderite collapses sharply across spin transition and bulk modulus changes. However, thermal conductivity, which could control the thermal structure in Earth’s interior and is related to the elastic properties of Fe-bearing carbonates, remains rarely studied. In this work, we study the vibrational spectrum and thermal conductivity of siderite along a-axis and c-axis form ambient condition to 65GPa under room temperature by Raman spectroscopy and Time-domain thermoreflectance combined with diamond anvil cell techniques. We found that the range of spin transition is 46GPa~52GPa, which is similar to previous studies, suggesting that iron concentration in siderite has minor effect on the pressure range of spin transition. Preliminary results show that the thermal conductivity of siderite along a-axis decreases across spin transition.

Keywords: siderite, spin transition , thermal conductivity

Crystal structure of protoenstatite quenched to ambient temperature

*Masami Kanzaki[1]

1. Institute for Planetary Matereials, Okayama University

Protoenstatite ($MgSiO_3$) is generally thought that it cannot be quenched to ambient temperature, however, there are several reports on quenched protoenstatite (e.g., Lee and Heuer, 1987). We also observed protoenstatite using ^{29}Si MAS NMR spectroscopy of $MgSiO_3$ sample taken out from a furnace and cooled down (Xue et al., 2002). However, there is no study on crystal structure of quenched protoenstaite nor quantitative analysis on proportion of enstatite polymorphs in the quenched samples. In this study, four samples with different cooling rates were studied by powder X-ray diffraction and micro-Raman spectroscopy.
Starting enstatite sample was prepared from reagent-grade MgO and SiO_2, and they were mixed, and pelletized, and treated at 1500 °C twice. In previous reports (Lee and Heuer, 1987; Reynard et al., 2008), glass or melt was quenched to obtain protoenstatie, but in the present study, ordinary solid state synthesis method was employed. The starting material was kept at 1500 °C for 5H, and cooled down to ambient temperature with four different cooling rates (150 K/h, 15H/h, taken out from the furance and bottom of Pt crucible was dipped into water, sample directly dipped into water). It is known that protoenstatite would transform to low-clinoenstatite by grinding. So the samples were handled gently. Since recovered samples were powder, no special treatment was necessary to put intho sample holder for powder X-ray diffraction measurement. Grain size of all samples are similar, and are about 5 micrometer with angular shapes. The Rietveld method was used to refine crystal structure of protoenstatite, and quantitative analysis of the samples (RIETAN-FP program used). For Raman spectroscopic measurement, recipe proposed by Reynard et al. (2008) is used to identify enstatite polymorphts.
From X-ray diffraction, it was found that all samples contain both protoenstatite and low-clinoenstatite. Their existence was also confirmed by micro-Raman spectroscopy including the starting material. Structural refinement was conducted using protoenstatite-rich sample. Obtained lattice parameters are consistent with extraporated values of high-temperature data (Jiang et al., 2002), suggesting no major structural change with temperature. Refined crystal structure of protoenstatite is essentially same as that determined at high temperature, and is consistent with similated structure using the DFT calculation (at 0 K). Quantitative analysis by the Rietveld method revealed that about 40% protoenstatite exists in Pt crucible bottom dipped into water sample, and about 30% for slowly cooled sample (15 K/h), and there is cooling rate dependence for the proportion. However, supposedly most rapidly quenched sample, directly dipped into water, showed lowest proportion (30%).
Present study revealed that even using common synthesis technique, significant amount of protoenstatite is remained in so-called low-clinoenstatite sample. This implys that previous phase equilibrium studies of the $MgSiO_3$ system might used such samples, and reassesment of those studies may be necessary. As a such example, a possiblitiy of incorrect phase relation between low-clinoenstatite and orthoenstatite due to overlooked protoenstatite will be discussed.

Jiang, D. et al. (2002) J. Min. Petrol. Sci., 97, 20
Lee, W.E. and Heuer, A.H. (1987) J. Am. Ceram. Sco., 70, 349
Reynard, B. et al. (2008) J. Euro. Ceram. Soc., 28, 2459
Xue, X. et al. (2002) Geochim. Cosomochim. Acta, 66, A853

Keywords: crystal structure of protoenstatite, quantitative analysis by Rietveld method, enstatite phase relation

Measurements of fusion enthalpy of anorthite and diopside by combining techniques of drop calorimetry and solution calorimetry

*Toru Sugawara[1], Toshiaki Ohirra[1]

1. Graduate School of Engineering Science, Akita University

Enthalpy of fusion of rock-forming minerals is required to calculate enthalpy of multicomponent silicate liquid and are of considerable importance in thermodynamic consideration and phase equilibrium calculation in igneous process. Fusion enthalpy of diopside has been measured by various methods. In contrast, few study has been reported an enthalpy of fusion of anorthite. We developed a twin conduction calorimeter and determined enthalpies of fusion of diopside and anorthite by combining drop calorimetry for molten diopside and anorthite and solution calorimetry for glasses.

First, differences of enthalpy of diopside and anorthite liquids between 1873-1773K and 273K were measured by drop calorimetry. Enthalpies of solution of the drop quenched glasses, anorthite glass annealed at 1100K for 72h and synthetic crystals of diopside and anorthite were determined by a hydrofluoric acid solution calorimetry. Measuring system of twin conduction calorimeter consists of sample and reference Teflon vessels placed on copper block and is immersed in a water thermostat. Approximately 50mg sample powders were reacted with 23wt% hydrofluoric acid solution, and then temperature difference of solution between both vessels was measured by thermistors. Enthalpy was calibrated by heating a resistance element.

Enthalpy of vitrification determined from difference of enthalpies of solution for quenched glass and crystal are 87.3±7.0 kJ/mol for diopside and 83.4±6.5kJ/mol for anorthite. Enthalpy of fusion at melting point was calculated from the enthalpy of vitrification, relative enthalpy measured by drop calorimetry and published heat capacity of minerals. The enthalpy of fusion determined for diopside is 138.7±7.0kJ/mol at 1665K and is consistent with values reported in previous four studies (137-139kJ/mol). The enthalpy of fusion of anorthite at melting point (1830K) is 145.0±6.5kJ/mol and 146.1±7.5kJ/mol when enthalpies of solution for quenched and annealed glasses are used, respectively. This is 10% higher than a value reported by Richet et al. (1984) (137.0±7.0kJ/mol). This discrepancy is probably caused by error in fictive temperature of glass sample used in solution calorimetry estimated in previous study.

Keywords: Silicate melt, Enthapy of fusion, Enthalpy of solution, Calorimetry

In situ hot/cool-stage AFM study on crystal growth of barite at 10 - 40°C

Wen Liu[2], *Yoshihiro Kuwahara[1], Keisuke Ootsuka[2], Masato Makio[2]

1. Faculty of Social and Cultural Studies, Kyushu University, 2. Graduate School of Integrated Sciences for Global Society, Kyushu University

Most global-scale geochemical phenomena begin with atomic-scale growth and dissolution reactions at the mineral-water interface. In situ Atomic Force Microscopy (AFM) allows direct observation of the growth and dissolution processes at the mineral-water interface at the site or step level. Many in situ and ex situ AFM studies on the dissolution reactions of the barite (001) surface have been conducted to elucidate the processes involved and problems mentioned above. However, to our knowledge, no in situ AFM study on mineral growth at low temperatures (below room temperature) has been reported. The dearth of low-temperature studies most likely owes to difficulties in constructing the AFM experimental system. Here we report the results of a experiment performed by in situ hot/cool-stage AFM observations of the growth behavior on the (001) surface of barite in supersaturated $BaSO_4$ solutions at 10 - 40°C.
The mechanism of crystal growth of barite was characterized by the spiral growth mechanism where rhombic growth spirals elongated along the [010] direction were formed and the two-dimensional (2D) nucleation mechanism in which circular sector-shaped two-dimensional (2D) nuclei were formed and developed. In addition, the adhesive growth mechanism was observed only at 10°C.
The kinetic laws of the crystal growth on the barite (001) surface differed among crystallographic directions and crystal growth mechanisms. The advance rates of the two steps of 2D nuclei were proportional to the *SI*. In contrast, the advance rates of the parallel steps with extremely short step spacing on growth spirals were proportional to SI^2, indicating that the lateral growth rates of growth spirals were directly proportional to the step separations. This dependence of the advance rate of every step on the growth spirals on the step separations predicts that the growth rates along the [001] direction of the growth spirals were proportional to *SI* for higher supersaturations. The nucleation and growth rates of the 2D nuclei increased sharply for higher supersaturations using exponential functions. Only at 10°C, these rates changed to be proportional to *SI* for higher supersaturateions, indicating a change in main crystal growth mechanism from the 2D nucleation to the adhesive growth one. Two critical supersaturation points corresponding to the changes in main crystal growth mechanisms from the spiral growth, via 2D nucleation, to adhesive growth tended to decrease with decreasing of solution temperature.

Keywords: Barite, Crystal Growth, AFM

Characteristic local structures of Ca, Ti, Fe were observed in fusion glass of shergottite

*Tsubasa Tobase[1,2], Akira Yoshiasa[1], Massimo Nespolo[2], Hidetomo Hongu [1], Hiroshi Isobe[1], Maki Okube[3], Hiroshi Arima[3], Kazumasa Sugiyama[3]

1. Graduate School of Science, Kumamoto University, 2. Université de Lorraine, CRM2, UMR 7036, 3. Institute of Materials Research, Tohoku University

Shergottite is a kind of martian meteorite. Shergottite has the special glass structures which were melted at entering the Earth’ s atmosphere. The special metamorphism was observed in the local structures of melting glass which were affected by high temperature and rapid cooling at entering the Earth’ s atmosphere (Tobase et al., 2016). In order to obtain the information about coordination number, atomic distance and valence state at each ions, we performed local structural analysis of Ca, Ti, and Fe in shergottite by XAFS method. The estimation of environment at entering the Earth’ s atmosphere and getting out of the Mars were performed by local atomic structural analysis. In this study, the formation environment of melting glass is analyzed by comparison of local structures between those in shergottite and natural impact-related glass.

On the basis of the shape of XANES spectra in shergottite, local structures of Ca in shergottite are almost similar to those in tektite and meteorite fusion glass, although slight difference in XANES spectra is observed. This slight difference might come from the chemical composition and coordination environment. The similarities in XANES spectra between shergottite and the other fusion glasses indicate that formation environment of fusion glass in shergottite is almost similar to that in the other meteorite. Okudera et al., (2012); Wang et al., (2013) reported that the main peak position in Fe XANES spectra is related to valence state such as oxidation state of Fe ions, which was influenced by the surrounding oxygen during formation process. The main peak position of Fe XANES spectra in shergottite is similar to those in the other fusion glasses, thus fusion glass in shergottite was estimated to be formed under the Earth’ s atmosphere like the other fusion glasses. On the other hand, local structural information of Ti in shergottite is different trend to that in Ca and Fe. Since the Ti XANES spectra in shergottite is similar to those in darwin glass whose formation condition is different from the other impact-related glasses and fusion glasses, fusion glass in shergottite might be experienced unique formation process. Shergottite which originated from the Mars contains the fusion glass produced during entering the Earth’ s atmosphere and glass part influenced during getting out of the Mars. The local structure in fusion glass of unique and different from the other fusion glasses.

Reference

Tobase et al., (2016), IOP Conference series, 712, 012095.
Wang et al., (2013), J. Miner. Petro. Sci., 108, 288-294.
Okudera et al., (2012), J. Miner. Petro. Sci., 107, 127-132.

Keywords: Shergottite, Local structure of Ca, Ti, Fe, XANES, EXAFS, Fusion glass

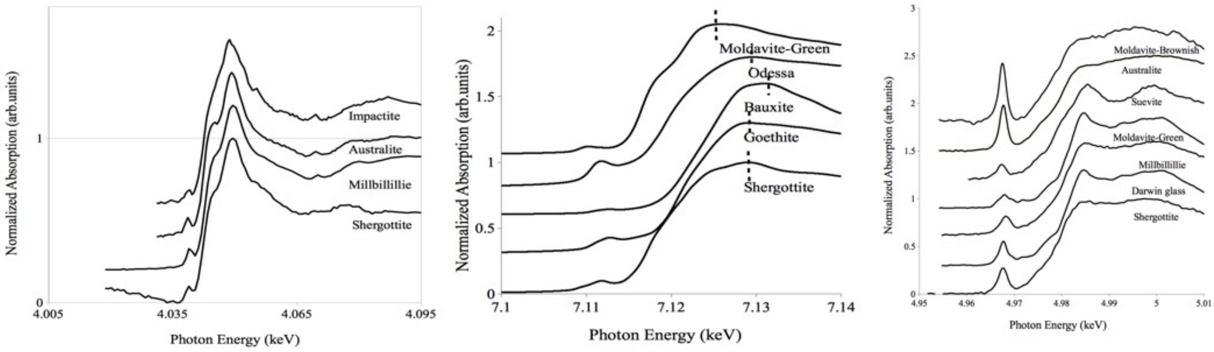

(a) Ca XANES spectra (b) Fe XANES spectra (c) Ti XANES spectra

Anomalous characteristics of relative formation and reaction for terrestrial mineral crystals

*Yasunori Miura[1]

1. Visiting (Yamaguchi, Foreign University (AIC University))

Mineral crystals are stored as databases in a global description with the physicochemical and earth science unit of rocks. However, description by identification of the minerals is based on the present environment through many solidified processes on active planet, where crystalline minerals reveal environmental indicator of different stages of planet Earth, together with extraterrestrial rocks originated from the Moon , Asteroids and Mars. The purpose of the present study is that minerals formed at successive planet Earth with different stages are applied to be compared with different environments of the primordial Earth and extraterrestrial bodies (with global water system or not) as follows.

1. Minerals formed on the active water planet Earth have environmental information on the time and place of generation and change and the place with different structure and composition in details. Therefore, the minerals formed on active planet Earth are all different physicochemical information without any representative mineral characteristics, but shown as only simple mineral names with bulk data.
2. Minerals formed on the Earth at different reaction time of the geological units have the same mineral name, but their physicochemical information is basically different, because of different environmental conditions to be formed on Earth.
3. If we can use same mineral names both in Earth and extraterrestrial bodies, precise compositional and structural data of minerals formed on active air- and water-planet Earth are precisely different. Therefore, any minerals formed on primordial Moon and planets without detailed material-database do not suggest past existence of global water on the extraterrestrial bodies of the Solar System.
4. The present study suggests that the minerals in the Earth are considered to be solidified remnants after evaporated and fluid processes without location of atomic sites and layer molecules, which are developed further to deep interior of largere planetary bodies.
5. Author would present the data in the JpGU-AGU 2017 meeting that the remained solids by quenched processes of the carbon-bearing grains of various Earth, Asteroids and lunar rocks showing the idea and the nano-technical images by the analytical electron microscopy relatively.
6. Elements (carbon) of volatile quench solidified material (carbon inclusions) formed in the impact process are decomposed to form the surface element-resources (diamond carbon etc.) on shallow surface to deep interior on active Earth, where real origins of the internal volatile elements of the deeper mantle rocks are relatively difficult to be determined for large planetary bodies only from present location site (esp. on many developments of deeper products).

7. The present results show that carbon-bearing solidified grains by quenching are remained at all shocked events of active young Earth and primitive extraterrestrial celestial bodies widely. When we can found carbon-bearing grains in primordial satellites and planets, they are continued to keep original grains without global ocean-water system of Earth-type planets clearly as one of new results in this study of the JpGU-AGU meeting 2017.

Keywords: Earth's minerals, Quenched solids with volatiles, Various mineral characteristics

CLAY MINERALOGY OF ALTERED VOLCANIC ASH BEDS AND FACIES CORRELATION BETWEEN THE PERMIAN TO TRIASSIC BOUNDARY STRATIGRAPHIC SETS IN GUIZHOU AND SICHUAN PROVINCE OF SOUTH CHINA

*Ni na Gong[1], qian Fang

1. China University of Geosciences

Permian to Triassic is the important stage for the Earth from Paleozoic to Mesozoic, and the extinction among the Permian to Triassic is a hot topic by researchers. Many researchers had been study it by different aspect. The view of volcanism to P-T extinction was accepted to more and more researchers, and the wide distribution of Permian to Triassic nearby boundary is the important record of extinction. The mineralogy characteristic of clay mineral can provide important information of sedimentary source, and the research about it has important research significance. Successions of the Permian-Triassic boundary (PTB) altered volcanic ash beds exist in south China.

The Permian-Triassic boundary (PTB) successions in south China contain numerous altered volcanic ash beds (K-bentonites), which presents the opportunity to correlate the PTB position in both marine and non-marine PTB sections. Clay mineralogical and geochemical studies of two altered ash beds in the Chahe(CH), in Guizhou Province and Shangsi (SS) in Sichuan Province sections, in south China, deposited in littoral and interactive marine-terrestrial environments respectively, permit an investigation of the alteration of ashes and correlation of ash beds between disparate facies. The results show that the two CH altered ashes are dominated by R2 and R3 I/S clays, with 86.3 % and 84.04 % illite layers for samples SS and 57.83 % and 68.19% illite layers, respectively. The CH ash samples contain mainly kaolinite and mixed-laye illite/smectite (I/S) clays. The poorly-crystallized kaolinite is present in pseudo-hexagonal plates, and the well-crystallized kaolinite occurs in book-like aggregates in veins or cavities. Obviously, the CH ashes experienced terrestrial weathering and resedimentation prior to final burial and preservation, and local microenvironmental conditions control the formation of clay minerals. The SS ash samples have markedly lower $^{87}Sr/^{86}Sr$ values (0.721708 for SS-1 and 0.717225 for SS-2) than those of the CH samples (0.761077 and 0.742332). The notable difference in $^{87}Sr/^{86}Sr$ value of ash beds between the sections is attributed to variations in Rb-Sr partitioning during the chemical weathering process in different environments. The CH ash samples have notably higher $^{149}Nd/^{144}Nd$ ratios (0.512376 for CH-1 and 0.512424 for CH-2) than those of the SS samples (0.512034 for SS-1 and 0.512043 for SS-2), suggesting that the CH ashes are likely derived from continental crust and the SS ashes originate from new continental island arcs, in agreement with the REE distributions and the Ti *vs*. Zr, TiO_2 *vs*. Al_2O_3, and Zr/TiO_2 *vs*. Nb/Y discrimination plots. The occurence of different volcanisms in PTB stratigraphic sets previously believed to be synchronous, south China, suggests that correlation between disparate facies by an ash marker is unwise without geochemical fingerprinting of the materials.

Keywords: Altered volcanic ash, illite-smectite, Sr isotopic composition, Nd isotopic composition, weathering

Understanding the origin of polycrystalline diamond, carbonado through analysis of nano-inclusions

*Hiroaki Ohfuji[1], Natsuko Asano[1], Hiroyuki Kagi[2]

1. Geodynamics Research Center, Ehime University, 2. Graduate School of Science, University of Tokyo

Carbonado is a type of polycrystalline diamond, which shows a grayish to black color and a massive and irregular morphology with a porous internal texture. It is distinct from ordinary mantle-derived diamonds in the following respects: extremely low carbon isotope composition (-25˜-30 ‰), absence of mantle-derived primary inclusions, high concentration of radiogenic noble gases, etc. Therefore, the origin of carbonado has long been controversial. A recent study (Ishibashi et al., 2010) found several lines of evidence that H_2O-rich fluid is present within constituent diamond grains of carbonado, suggesting its formation in close association with C-H-O fluid in the Earth’ s mantle. However, the detail of the formation process and condition of carbonado is still unclear.
Here, we found, for the first time, primary mineral inclusions (majoritic garnets, phengite, rutile, apatite, etc.) in nano-sized negative crystals within diamond grains by detailed FE-SEM and TEM observations. Those precipitates usually occur as an assemblage of a few to several mineral phases that are mostly in euhedral forms in the negative crystals. They are most likely quenched products from silicic fluid that were trapped during the crystal growth of diamonds that comprise carbonado. The presence of these mineral phases in negative crystals suggests that the formation of carbonado occurred in fluid-saturated environments to which crustal materials (e.g. basalt) are supplied potentially by the subduction of oceanic plates or extensive collision of continental plates to form a thick mantle keel.

Keywords: Diamond, Carbonado, inclusion

CaO_8 and MgO_8 clustering in $Grs_{50}Prp_{50}$ garnet in diamond-bearing dolomite marble from the Kokchetav Massif

*Tomohiro Takebayashi[1], Takeaki Saito[2], Kunihiko Sakamaki[1], Hiroshi Suzuki[2,1], Yoshihide Ogasawara[2,1]

1. Department of Earth Sciences, Resources and Environmental Engineering, Graduate school of Creative Science and Engineering, Waseda University, 2. Department of Earth Sciences, Waseda University

Grossular-pyrope garnet (ca. $Grs_{50}Prp_{50}$) has long been attracted about crystal chemistry, mixing properties, and P-T stabilities. Many experimental and thermodynamic studies on grossular-pyrope garnet have been conducted (e.g., Ganguly et al., 1996; Geiger, 2013; Du et al., 2016). Garnet having near the $Grs_{50}Prp_{50}$ composition is extremely rare in nature. Only two occurrences have been reported, so far; (1) xenocrysts in the kimberlite from Garnet Ridge, Arizona (Wang et al., 2000) and (2) diamond-bearing dolomite marble from the Kokchetav UHP Massif, Kazakhstan (e.g., Ogasawara et al., 2000; Sobolev et al., 2001). This strange garnet from the Kokchetav Massif is a main constituent silicate mineral of dolomite marble (P > 6 GPa, T = ca. 1000 ˚C) and is a main host mineral of abundant microdiamond (Ogasawara et al., 2000; 2005). This garnet is chemically homogeneous and has its composition range: Grs: 43-46, Prp: 39-42, and Alm: 10-16 mol%. The closest composition to $Grs_{50}Prp_{50}$ is $Grs_{44}Prp_{42}Alm_{10}$. No exsolution and no symplectite were observed.
We conducted laser Raman spectrometry on this $Grs_{50}Prp_{50}$ garnet in the Kokchetav UHP dolomite marble. Among the obtained Raman bands at 366, 556, and 903 cm^{-1}, we focused on the band at 366 cm^{-1} that was assigned to $R(SiO_4)^{4-}$. FWHM of this band was significantly large (24.5 cm^{-1}), compared to those of Prp (14.3 cm^{-1}at 365 cm^{-1}) and Grs (14.0 cm^{-1} at 372 cm^{-1}). Such a large FWHM of $Grs_{50}Prp_{50}$ garnet suggested that two kinds of $R(SiO_4)^{4-}$ bands corresponding to Grs and Prp were obtained as one overlapped broad band because the peak positions of both bands are very close. The synthesized band from Grs and Prp end-member was well fitted to the observed band.
In the crystal structure of garnet, a SiO_4 tetrahedron is surrounded by six dodecahedra XO_8 (Geiger, 2013). A SiO_4 tetrahedron of grossular surrounded by six CaO_8, and that of pyrope by six MgO_8. The observed overlapping of two $R(SiO_4)^{4-}$ bands corresponding to Grs and Prp indicates two modes for $R(SiO_4)^{4-}$ in a single $Grs_{50}Prp_{50}$ crystal; $R(SiO_4)^{4-}$ of SiO_4 surrounded by six CaO_8 (CaO_8 clustering around SiO_4) and that by six MgO_8 (MgO_8 clustering around SiO_4). Such clustering stabilized garnet of ca. $Grs_{50}Prp_{50}$, and could be controlled by two factors: (1) bulk chemistry near Ca:Mg = 1:1 and (2) UHP conditions. No exsolution lamella and no symplectite mean that $Grs_{50}Prp_{50}$ garnet was stable under low P and T once it formed at high P and T.

Reference

Du, W., Clark, S.M., Walker, D., 2016, *American Mineralogist*, **101**, 193-204.
Ganguly, J., Cheng, W., Tirone, M., 1996, *Contributions to Mineralogy and Petrology*, **126**, 137-151.
Geiger, C.A., 2013, *Elements*, **9**, 447-452.
Ogasawara, Y., 2005, *Elements*, **1**, 91-96.
Ogasawara, Y., Ohta, M., Fukasawa, K., Katayama, I., Maruyama, S., 2000, *Island Arc*, **9**, 400-416.
Sobolev, N.V., Schertl, H.-P., Burchard, M., Shatsky, V.S., 2001, *Doklady Earth Science,* **380**, 791-794.
Suzuki, H., Takebayashi, T., Saito, T., Sakamaki, K., Ogasawara, Y., 2017, *JpGU Meeting* abstract.
Wang, L., Essene, E.J., Zhang, Y., 2000, *American Mineralogist*, **85**, 41-46.

Keywords: Grossular-Pyrope Garnet, Ultrahigh-pressure, diamond, Laser Raman spectroscopy, clustering, Kokchetav

A new insight on the chloritization mechanism of biotite in hydrothermally altered granite

*Takahiro Ishii[1], Toshihiro Kogure[1], Ryosuke Kikuchi[1], Ritsuro Miyawaki[2], Takashi Yuguchi[3]

1. University of Tokyo, 2. National Museum of Nature and Science, 3. Yamagata University

Chlorite commonly forms by hydrothermal alteration of biotite in granitic rocks. This “chloritization” mechanism of biotite has been paid attention and investigated for a long time to understand alteration history of granitic rock which is one of the most common lithofacies. However, it looks that previous studies have focused either crystallographic [1, 2] or chemical aspect [3] of the chloritization, not both. This study investigated the chloritization process of biotite, by analysing both the crystal structures and chemical compositions of the chlorite. As a result, a new insight for the chloritization, simultaneous occurrence of the two transformation mechanisms, is proposed.
The rock investigated was Toki granite, distributed in Central Japan. The sample was collected from the borehole in the Mizunami Underground Research Laboratory; in the altitude range from -274m to -314 m above sea level [3]. Observation of the petrographic thin sections revealed that the granite contains biotite with various stages of chloritization. Generally, biotite grains of various chloritization are homogeneously distributed in a thin section. X-ray diffraction (XRD) patterns obtained using a Gandolfi camera confirmed that the dominant polytype of unaltered biotite is 1*M* and the polytypic group of the emerald-like coloured chlorite grains is II*bb*. Electron microprobe analysis revealed that emerald-like coloured, completely chloritized grains contain no titanium (Ti) which is a constituent element of biotite in granite (“Ti-free chlorite”). On the other hand, element mapping of partially chloritized biotite grains indicated that the grains contain thin regions with no potassium (namely no biotite component) but with a certain amount of Ti. Considering existence of other elements, these thin regions are also considered to be chlorite (“Ti-bearing chlorite”). Quantitative analysis of these Ti-free and Ti-bearing chlorite showed different Al contents and Mg/Fe ratios between them, beside the amount of Ti. Investigation using TEM confirmed that both Ti-free and Ti-bearing chlorites are really “chlorite”, from electron diffraction and high-resolution imaging.
This compositional difference can be ascribed to different chloritization mechanisms; Ti-bearing chlorite took over the 2:1 layer from biotite, and Ti-free chlorite was formed via dissolution-recrystallization process. In biotite, Ti is expected to locate in the octahedral sheet of the 2:1 layer. Hence, chlorite transformed from biotite must contain Ti, if the 2:1 layer was inherited from biotite without significant cation diffusion. On the contrary, chlorite can be Ti-free, if the 2:1 layer was once dissolved and new 2:1 layers formed from the hydrothermal fluid. In this case, Ti formed titanite, $CaTiSiO_5$, which is common within chloritized grains, with calcium and silicon transported via the fluid. In TEM, Ti-bearing chlorite showed a diffraction pattern indicating a mixture of different polytypic groups, indicating structural discontinuity with completely chloritized grains which were II*bb* from XRD. II*bb* is considered to be the most stable polytypic group and expected to form if chlorite was formed from solution. However, if chlorite was transformed from biotite via a solid-to-solid pathway inheriting the 2:1 layer, complete II*bb* stacking may not be expected owing to the difference of the interlayer structures between biotite and chlorite [2]. Finally, high-resolution imaging support that Ti-bearing chlorite inherited the 2:1 layer from biotite, because this chlorite has 2:1 layers whose orientation is uniform, which is the same characteristic as biotite-1*M*. On the other hand, Ti-free chlorite consists of 2:1 layers whose orientation is considerably disordered.

[1] Veblen DR., Ferry JM. (1983). A TEM study of the biotite-chlorite reaction and comparison with

petrologic observations. American Mineralogist, 68, 1160-1168.
[2] Kogure T., Banfield JF. (2000). New insights into the mechanism for chloritization of biotite using polytype analysis. American Mineralogist, 85, 1202-1208.
[3] Yuguchi T., Sasao, E., Ishibashi M., Nishiyama, T. (2015). Hydrothermal chloritization process from biotite in the Toki granite, Central Japan: Temporal variations of the compositions of hydrothermal fluids associated with chloritization. American Mineralogist, 100, 1134-1152.

Keywords: chloritization, biotite, hydrothermal alteration, granite

$Grs_{50}Prp_{50}$ garnet-bearing composite inclusion in Cr-rich pyrope from Garnet Ridge, the Colorado Plateau

*Hiroshi Suzuki[1,2], Tomohiro Takebayashi[2], Takeaki Saito[1], Kunihiko Sakamaki[2], Yoshihide Ogasawara[1,2]

1. Department of Earth Sciences, Waseda University, 2. Department of Earth Sciences, Resources and Environmental Engineering, Graduate school of Creative Science and Engineering, Waseda University

Garnet having near $Grs_{50}Prp_{50}$ composition is very rare in nature because of the large difference in ionic radii between Ca^{2+} and Mg^{2+}. So far, only two occurrences have been reported from Garnet ridge, Arizona (Wang *et al*., 2000) and the Kokchetav UHP Massif, Kazakhstan (e.g., Ogasawara *et al*., 2000; Sobolev *et al* ., 2001). At Garnet Ridge, Wang *et al*. (2000) described four grains of $Grs_{50}Prp_{50}$ garnet as a constituent of composite inclusions in pyrope-rich garnet in kimberlitic diatremes. In the Kokchetav UHP Massif, $Grs_{50}Prp_{50}$ garnet is a major constituent mineral of UHP dolomite marble, and contains abundant microdiamonds. Takebayashi *et al*. (2017) has stated that CaO_8 and MgO_8 clustering around a SiO_4 tetrahedron stabilized ca. $Grs_{50}Prp_{50}$ compositions on the basis of the overlapping of $R(SiO_4)^{4-}$ Raman bands corresponding to Grs (372 cm^{-1}) and Prp (364 cm^{-1}), and considered that two main factors controlled the formation of this strange garnet; (1) the bulk chemistry of the host rock (Ca:Mg = 1:1) and (2) UHP conditions.

Recently, we discovered one grain of $Grs_{50}Prp_{50}$ garnet from the Garnet Ridge; the garnet occurs as a constituent of composite inclusion in the host Cr-rich pyrope (Group A by Sakamaki *et al*., 2016), which is of garnet lherzolite origin. Cr-rich pyrope (Group A) is an original material for Cr-poor pyrope (Group B) during mantle metasomatism. The found composite inclusion, which shows spherical form measuring 150 mm across, consists of pargasite and dolomite with minor Cr-spinel, phlogopite and apatite. The other composite inclusions consist of pargasite, dolomite, Cr-spinel with minor apatite and magnesite. We conducted laser Raman spectrometry on this $Grs_{50}Prp_{50}$ garnet, and focused on the band attributed to $R(SiO_4)^{4-}$ at 365 cm^{-1}. The overlapping of $R(SiO_4)^{4-}$ bands corresponding to Grs and Prp in a single $Grs_{50}Prp_{50}$ crystal was observed. Our results of Raman spectrometry were consistent with those of the Kokchetav $Grs_{50}Prp_{50}$ garnet by Takebayashi *et al*. (2017).

Almost all composite inclusions contain dolomite/magnesite and show rounded or spherical form. This suggests that these composite inclusions was trapped carbonate-silicate melt during the mantle metasomatism. The $Grs_{50}Prp_{50}$ garnet in the found composite inclusion was formed from such trapped melt which had the bulk chemistry, near Ca:Mg = 1:1, at very high pressure.

The $Grs_{50}Prp_{50}$ garnet described by Wang *et al*. (2000) could have formed by the same process from trapped carbonate-silicate melt, and the inclusion $Grs_{50}Prp_{50}$ garnet was not in equilibrium with the host pyrope-rich garnet. Their interpretation about the genesis of $Grs_{50}Prp_{50}$ garnet including very low formation temperature based on the coexistence with the host may be wrong.

.

References

Ogasawara, Y., Ohta, M., Fukasawa, K., Katayama, I., Maruyama, S., 2000, *Island Arc*, **9**, 400-416.
Ogasawara, Y., Sakamaki, K., Takebayashi, T., Suzuki, H., Saito, T., 2016, *AGU Fall Meeting*, SR33A-2673.
Sakamaki, K., Sato, Y., Ogasawara, Y., 2016, *Progress in Earth and Planetary Science*, **3**, 1-17.
Sobolev, N.V., Schertl, H.-P., Burchard, M., Shatsky, V.S., 2001, *Doklady Earth Science*, **380**, 791-794.
Takebayashi, T., Saito, T., Suzuki, H., Sakamaki, K., Ogasawara, Y., 2017. *JpGU Meeting Abstract.*
Wang, L., Essene, E.J., Zhang, Y., 2000, *American Mineralogist*, **85**, 41-46.

Keywords: Grossular-pyrope garnet, Garnet Ridge, Kimberlite, Laser Raman spectroscopy, Colorado Plateau, Cr-rich pyrope